Time-Domain Microwave Breast Cancer Detection: Experiments with Comprehensive Glandular Phantoms

Emily Porter, Adam Santorelli, Alexandre Bourdon, Dady Coulibaly, Mark Coates, Milica Popovi

Department of Electrical and Computer Engineering, McGill University
Montreal, Canada
{emily.porter, adam.santorelli, alexandre.bourdon, dady.coulibaly}@mail.mcgill.ca
{mark.coates, milica.popovich}@mcgill.ca

***Abstract* — This paper presents measurements performed on glandular phantoms using a time-domain microwave breast cancer detection system. The breast phantoms used in testing the system have skin-, fat-, glandular- and tumor-mimicking tissues with dielectric properties similar to those of actual tissues. This work provides the steps to composing a phantom with appropriate glandular structures, and to building breast phantoms with different percentages of glandular tissue. Finally, we present measurements from the tumor detection system with the breast phantoms in place.**

***Index Terms* — cancer detection, microwave imaging, microwave propagation, phantoms.**

I. Introduction

Microwave imaging for breast cancer detection is an area of research that is currently receiving a lot of interest. It has promise to become a complementary modality to common detection techniques, such as x-ray mammography. While the use of x-ray mammography is widespread, it has been shown to suffer high false-negative and false-positive rates [1], [2]. Since early detection is a key factor in reducing breast cancer fatality rates [3], investigating methods to supplement mammography is desirable. Microwave imaging is one such method, based on the inherent contrast in the dielectric properties of healthy and tumorous breast tissues over the microwave frequency range. It would be non-invasive, and is thought to be a safe, pain-free way to image the breast. Further, in contrast to mammography, microwave techniques do not use ionizing radiation [2].

This paper uses a time-domain microwave breast cancer detection system, previously described in [4], to detect malignant growths within the breast. The goal of our work is a system that can be applied to a doctor-certified healthy patient and then thereafter at prescribed intervals to identify if any irregular changes in breast composition have occurred. Thus, we aim not to fully reconstruct a dielectric profile of the breast, but rather to signal 'yes' or 'no', indicating if breast changes are suspicious and further testing should be undergone.

Here, we present tests of our system's tumor detection capabilities with breast phantoms that are as realistic as possible in terms of their tissue composition, organization, and electrical properties. To our knowledge, the literature offers no examples of high-level (both in terms of dielectric parameters and structure) breast phantoms. In contrast to our previous work in [4], [5], the test phantoms used in this work include the healthy tissues of skin, fat and gland, as well as a malignant tumor. More specifically, the measurements presented here explore how the presence of various amounts of glandular material within the breast affects the ability to detect the tumor response.

The next section describes the breast phantoms, with a specific focus on the steps involved in producing a phantom with appropriate glandular structures embedded in the fatty tissue. Following this, Section III details the experimental set-up. Section IV presents the measurement results for various tumor sizes and positions within the glandular breast phantoms, while Section V discusses the implications of these measurements.

II. Preparing the Phantoms

A. Tissue-Mimicking Phantom Mixtures

We simulate the four breast tissues of skin, fat, gland and tumor using common chemicals. The tissue phantoms are designed to have dielectric properties over the microwave frequency range that are similar to those of actual breast tissue measurements as reported in the literature [6]. The mixtures used for the tissue-mimicking phantoms are based on [7], research which also shows that placing individual tissue phantoms in contact with each other does not affect their original dielectric properties. In our previous work [8], we described our phantoms' chemical compositions, electrical properties, and the procedure for mixing; also explained is the procedure for making a complete heterogeneous breast phantom.

B. Gland Phantom Construction

In this work, we present three complete phantoms, each including the four tissue types. The phantoms have varying compositions of the fat and gland tissue types. The three models that are considered here are: 80% gland (20% fat), 50% gland (50% fat), and 30% gland (70% fat). For example, the first complete breast phantom has a skin layer, with an interior that is 80% gland and 20% fat, by volume.

The first step in making each phantom is creating the skin. The liquid skin-mimicking mixture is poured into a bowl-shaped mould designed specifically for the purpose of

generating a thin 2.5-mm hemi-spherical skin layer (outer radius of 6.5 cm). While the skin hardens, a mixture of gland phantom is poured into several conical shell moulds. There are two sizes of conical moulds, one with a volume of 27 mL and the other of 30 mL. An example of such a mould, and the gland phantom produced by it is shown in Fig. 1.

Fig. 1. Photograph of the hollow conical gland mould (bottom), and a sample of a gland structure produced by it (top).

The total volume enclosed by the skin layer is calculated, and then the amount to be filled with gland is determined from the desired percentage of gland within the tissue. A number of conical-shaped glands are used until the gland volume requirement has been satisfied. If, for instance, the necessary volume of gland is not a multiple of the gland-mould volumes of 27 mL and 30 mL, then these glands are simply trimmed to a shorter height, allowing any given volume to be created.

Once the glands are removed from their moulds they are placed within the hemi-spherical skin. The positioning is random with respect to gland size, and the glands are spread out symmetrically along the circumference of the skin. The 30% gland phantom only requires 7 conical gland structures, 3 of which have been trimmed smaller. The 50% gland model has 10 gland structures: 7 spread out along the skin wall and 3 around the phantom center. Finally, the 80% gland breast phantom is filled with 13 conical glands, 9 in an outer ring and 4 in the middle. Photographs of the semi-completed phantoms at this stage of construction are shown in Figs. 2-4 for breast phantoms with 30%, 50% and 80% gland, respectively.

After the glands have been placed inside the skin, the remaining space is filled with fat-mimicking tissue. This is the final step in making the breast model. However, a batch of tumor phantom must also be made at this time in order for it to be used in tumor detection measurements. The tumor mixture can be allowed to harden in any shape mould, and once it is set it is carved manually into the shape and size desired for the measurements.

III. Experimental Set-Up

Our past work [4] describes the experimental system in detail. Here, we provide a brief overview. The system consists of two UWB antennas called TWTLTLA (Travelling Wave Tapered and Loaded Transmission Line Antenna), described in [9]. The set-up as is follows: a specially designed hemi-spherical bowl-shaped radome holds the two antennas in slots along the exterior of it, and holds on its interior the breast phantom under test (surrounded by a fat-like matching medium to ensure no air gaps exist). The radome is a dielectric made of Alumina (Friatec, [10]), with $\varepsilon_r \bullet 9.6$. The radome allows for flexible antenna positioning, for instance, the co-polarized and cross-polarized responses can be measured for both transmission through the breast phantom and reflection back off it.

Fig. 2. Photograph of the partially completed 30% gland phantom, with 7 glandular structures.

Fig. 3. Photograph of the partially completed 50% gland phantom, with 10 glandular structures.

Fig. 4. Photograph of the partially completed 80% gland phantom, with 14 glandular structures.

Once we place the breast phantom in the radome and the antennas in their desired slots, an impulse generator (Picosecond Pulse Labs, [11], Impulse Generator Model 3600), activated by a clock at 25 MHz (Tektronix, [12], gigaBERT 1400 generator), sends a pulse to the transmitting antenna. The pulse is characterized by a -7.5 V amplitude

with full-width at half maximum of 70 ps. The transmitting antenna propagates the pulse through the radome and into the breast phantom, where it is scattered off all tissue interfaces. The receiving antenna, attached to a picoscope (Pico Technology, [13], PC Oscilloscope 9201) then records the transmitted or scattered signal from the breast phantom and saves it to the computer for further analysis.

In this particular series of experiments, we perform five sets of measurements on every test phantom, each one relating to a different antenna position. Table I presents the list of cases, where the case numbering is consistent with past work. For example, case 2 describes a situation in which the transmit and receive antennas are on opposite sides of the breast phantom, and are oriented perpendicularly. Thus, case 2 measures a transmission scenario, where the system records the cross-polarized response. Cases 5 and 6 appear the same in the table as only a slight change is made between them: swapping of the locations of the transmit and receive antenna.

TABLE I
LIST OF MEASUREMENT SCENARIOS

Case #	Polarization	Transmission or Reflection
1	Co-	Transmission
2	Cross-	Transmission
5	Co-	Reflection
6	Co-	Reflection
7	Cross-	Reflection

For each breast phantom, we use three sizes of tumors (one at a time) to test if the system is able to detect the tumor. The tumors are all approximately spherical, carved by hand, with diameters of 0.5 cm (small tumor), 1 cm (medium), and 2 cm (large). They are located within the phantom by slicing open a narrow section and inserting the tumor into the slice at the desired depth. In cases 1 and 2, we position the tumors directly at the centre of the breast phantom, between 0.5 cm and 1 cm from the chest wall. In cases 5-7, the tumors are halfway between the centre of the breast phantom and the radome wall where the antennas are located, with the tumor depth the same as in cases 1 and 2.

For each breast phantom, we test all 5 cases. Each case is composed of measurements with the 3 tumors in place, as well as a baseline measurement representing the healthy tissue. This leads to a total of 20 measurements for each phantom. We calculate the tumor response for each tumor as the difference between the healthy baseline and the response measured when the tumor is in place in the breast.

IV. RESULTS

We assess the quality of the signals obtained from the system through the calculation of two key metrics. The peak received signal, calculated as the maximum of the absolute value of the received signal, allows us to ensure the signal is clearly visible above the noise level of the equipment. The peak tumor response, similarly, tells us whether or not the tumor can be detected by the system. The peak tumor response is the maximum of the absolute value of the difference between the baseline signal and the received signal when the tumor is present.

As a sample of the measurements, Fig. 5 plots one period of each the received signal and the tumor response, for the 80% gland phantom, case 5, medium sized tumor. The tumor response is slightly noisier than the received signal, but in both plots the signal is clearly defined and above the noise level.

Finally, a summary of the measurement results is presented in Table II. This table shows the smallest peak tumor responses, across tumor sizes, for each breast phantom (30%, 50% and 80% gland), and for each of the 5 cases. In the table, 'N' refers to a signal that has no peak value because it is entirely engulfed by noise.

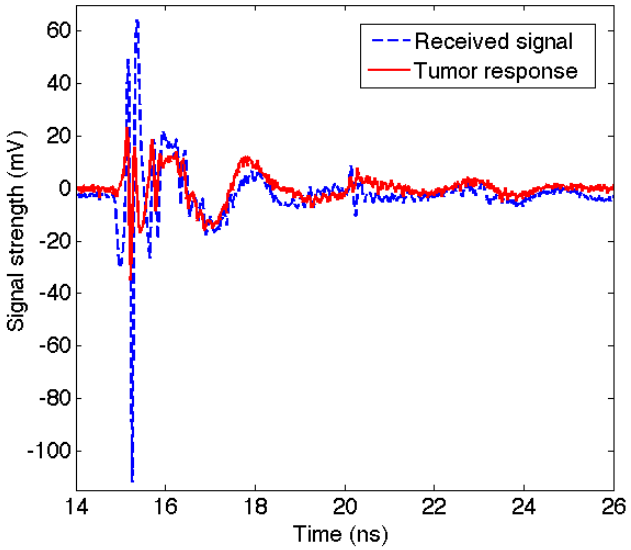

Fig. 5. Received signal (blue, dashed line) and tumor response (red, solid line) for 80% gland phantom, case 5, medium-sized tumor.

V. DISCUSSION

The results in Table II show that for phantoms with all percentages of glandular tissue, all three sizes of tumor can be detected by at least one of the five antenna arrangements. In fact, the system detects each tumor size in each phantom with at least three out of the five antenna cases. For 30%, 50% and 80% gland, case 2 leads to a tumor response that is not detectable above the noise level. This indicates that in a real-life detection system, a cross-polarized transmission signal is not the best choice for detecting tumors.

The measurements also demonstrate that a larger tumor does not necessarily provide a larger tumor response (from Table II, for example, the 30% gland phantom in case 6 with

a larger tumor gives a lower peak tumor response than both the medium and small sized tumors). This could be caused by the large tumor effectively blocking the signal from reaching the receive antenna.

TABLE II

SUMMARY OF MEASUREMENTS: MINIMUM PEAK TUMOR RESPONSE FOR 30%, 50% AND 80% GLAND PHANTOMS (TUMOR SIZE THAT GIVES THE MINIMUM PEAK TUMOR RESPONSE), FOR EACH CASE. 'N' REFERS TO THE SIGNAL BEING OBSCURED BY NOISE.

	Minimum peak tumor response (corresponding tumor size)		
	30% GLAND	50% GLAND	80% GLAND
Case 1	N	5 mV (small)	8 mV (small)
Case 2	N	N	N
Case 5	9 mV (small)	11 mV (small)	24 mV (small)
Case 6	15 mV (large)	11 mV (small)	16 mV (small)
Case 7	3 mV (medium)	3 mV (small)	23 mV (medium)

Also, the tumor response does not necessarily improve with decreasing amount of gland in the phantom (i.e., increasing fat content). Due to the layout of the glandular structures, sometimes they will affect the tumor response more negatively than other times (for instance if the gland is directly in front of the transmitting or receiving antenna).

Finally, we note that cases 5 and 6 provide consistently good tumor responses, for phantoms with all ratios of glandular to fatty tissue, and for all tumor sizes. These reflection-scenario cases consistently provide improved tumor responses over the transmission-scenarios of cases 1 and 2. This suggests that an acceptable detection performance may be obtained without performing the case 1 and 2 measurements.

VI. CONCLUSION

In this work, we tested the detection abilities of our time-domain microwave breast cancer detection system. Breast phantoms composed of skin, fat and varying levels of glandular tissue, with appropriate dielectric properties, were designed and constructed. Our system measured the tumor response for three sizes of tumors in each glandular breast phantom for five various antenna arrangements. We easily detect a tumor response for all tumors, in all of the breast phantoms. These results are promising and suggest that the ability of the time-domain system to identify a tumor is not seriously compromised by the presence of large amounts of glandular tissue.

ACKNOWLEDGEMENT

The authors are grateful for the funding support by the Natural Sciences and Engineering Research Council of Canada (NSERC), le Fonds québécois de la recherche sur la nature et les technologies (FQRNT), and Partenariat de Recherche Orientée en Microélectronique, Photonique et Télécommunications (PROMPT). The authors also thank Jules Gauthier of Polytechnique Montreal for fabricating our antennas, and Donald Pavlasek of McGill University for machining the mould used to create the skin phantom.

REFERENCES

[1] E.C. Fear, P.M. Meaney and M.A. Stuchly "Microwaves for breast cancer detection?" *IEEE Potentials*, pp.12-18, February/March 2003.

[2] I.J. Craddock, A. Preece, J. Leendertz, M. Klemm, R. Nilavalan and R. Benjamin, "Development of a hemi-spherical wideband antenna array for breast cancer imaging," in *Proc. 1st European Conference on Antennas and Propagation (EUCAP 2006)*, Nice, France, 6-10 November, 2006.

[3] American Cancer Society, "Cancer Facts & Figures," 2010.

[4] E. Porter, A. Santorelli, M. Coates r t e r . Popović, "An Experimental System for Time-Domain Microwave Breast Imaging," in *Proc. 5th European Conference on Antennas and Propagation (EUCAP 2011)*, Rome, Italy, April 11-15, 2011.

[5] E. Porter, A. Santorelli, M. Coates and M. Popović, "Microwave Breast Imaging: Time-Domain Experiments on Tissue Phantoms," in *Proc. 2011 IEEE International Symposium on Antennas and Propagation (AP-S 2011)*, Spokane, Washington, July 3-8, 2011.

[6] M. Lazebnik, D. Popovic, L. McCartney, C. Watkins, M, Lindstrom, J. Harter, S. Sewall, T. Ogilvie, A. Magliocco, T. Breslin, W. Temple, D. Mew, J. Booske, M. Okoniewski and S. Hagness, "A large-scale study of the ultrawideband microwave dielectric properties of normal, benign and malignant breast tissues obtained from cancer surgeries," *Phys. Med. Biol., Vol. 52, pp. 6093-6115, 2007.*

[7] M. Lazebnik, E. Madsen, G. Frank and S. Hagness, "Tissue-mimicking phantom materials for narrowband and ultrawideband microwave applications," *Phys. Med. Biol.,* Vol. 50, pp. 4245-4258, 2005.

[8] E. Porter, J. Fakhoury, R. Oprisor, M. Coates and M. Popović, "Improved Tissue Phantoms for Experimental Validation of Microwave Breast Cancer Detection," in *Proc. 4th European Conference on Antennas and Propagation (EUCAP 2010)*, Barcelona, Spain, April 12-16, 2010.

[9] H. Kanj and M. Popović, "A novel ultra-compact broadband antenna for microwave breast tumor detection" *Progress in Electromagnetics Research*, PIER 86, pp. 169-198, 2008.

[10] Friatec. (2011, May 3). [Online]. Available: http://www.friatec.com/

[11] Picosecond Pulse Labs. (2011, May 3). [Online]. Available: http://www.picosecond.com/

[12] Tektronix. (2011, May 3). [Online]. Available: http://www.tek.com/

[13] Pico Technology Limited. (2011, May 3). [Online]. Available: http://www.picotech.com/